Full length article

Optimally oriented grooves on dental implants improve bone quality around implants under repetitive mechanical loading

Shinichiro Kuroshima [a,*], Takayoshi Nakano [b], Takuya Ishimoto [b], Muneteru Sasaki [a], Maaya Inoue [a], Munenori Yasutake [a], Takashi Sawase [a]

[a] Department of Applied Prosthodontics, Graduate School of Biomedical Sciences, Nagasaki University, Nagasaki, Japan
[b] Division of Materials and Manufacturing Science, Graduate School of Engineering, Osaka University, Osaka, Japan

ARTICLE INFO

ABSTRACT

The aim was to investigate the effect of groove designs on bone quality under controlled-repetitive load conditions for optimizing dental implant design. Anodized Ti-6Al-4V alloy implants with $-60°$ and $+60°$ grooves around the neck were placed in the proximal tibial metaphysis of rabbits. The application of a repetitive mechanical load was initiated via the implants (50 N, 3 Hz, 1800 cycles, 2 days/week) at 12 weeks after surgery for 8 weeks. Bone quality, defined as osteocyte density and degree of biological apatite (BAp) c-axis/collagen fibers, was then evaluated. Groove designs did not affect bone quality without mechanical loading; however, repetitive mechanical loading significantly increased bone-to-implant contact, bone mass, and bone mineral density (BMD). In $+60°$ grooves, the BAp c-axis/collagen fibers preferentially aligned along the groove direction with mechanical loading. Moreover, osteocyte density was significantly higher both inside and in the adjacent region of the $+60°$ grooves, but not $-60°$ grooves. These results suggest that the $+60°$ grooves successfully transmitted the load to the bone tissues surrounding implants through the grooves. An optimally oriented groove structure on the implant surface was shown to be a promising way for achieving bone tissue with appropriate bone quality. This is the first report to propose the optimal design of grooves on the necks of dental implants for improving bone quality parameters as well as BMD. The findings suggest that not only BMD, but also bone quality, could be a useful clinical parameter in implant dentistry.

Statement of Significance

Although the paradigm of bone quality has shifted from density-based assessments to structural evaluations of bone, clarifying bone quality based on structural bone evaluations remains challenging in implant dentistry. In this study, we firstly demonstrated that the optimal design of dental implant necks improved bone quality defined as osteocytes and the preferential alignment degree of biological apatite c-axis/collagen fibers using light microscopy, polarized light microscopy, and a microbeam X-ray diffractometer system, after application of controlled mechanical load. Our new findings suggest that bone quality around dental implants could become a new clinical parameter as well as bone mineral density in order to completely account for bone strength in implant dentistry.

1. Introduction

Implant therapy has been one of the most secure and reliable treatments for ensuring the success and longevity of oral rehabilitation. Dental implants are constitutively subjected to repetitive

loads, including functional loads such as mastication and swallowing, and parafunctional loads such as clenching, grinding, and tapping movements. On the other hand, bone loss of less than 0.2 mm annually after the first year of the implant is necessary for therapeutic success [1]. Indeed, marginal bone loss around dental implants seriously disfeatures aesthetic profiles and hinders successful outcomes. One study using finite element analysis reported that load stress is concentrated mainly on the neck of bone around implants [2], and other studies have indicated that stress distribu-

tion is affected by differences in implant neck design [3–5]. In addition, some animal studies conducted to investigate the effects of bite force have reported that mechanical load affects the marginal bone level around dental implants [6–8]. Taken together, these previous findings suggest that the marginal bone architecture around implants is influenced by implant neck designs and mechanical load. However, because the amplitude, frequency, cycle and duration of bite force are difficult to control, little evidence has been reported regarding the net effect of implant design on bone around dental implants under appropriate load conditions.

Microthreads have been widely used in dental implants because of their ability to reduce marginal bone loss by enhancing mechanical stability between bone and implant [9]. Rough surfaces and microthreads promote stress anchoring and transmission at the bone/implant surface by increasing the bone/implant contact area [5]. Currently, several kinds of dental implants with microthreads in their neck are commercially available worldwide. However, bone quality around microthreads, which may be related to the mechanical stability of implants, has not been well documented, and microthread design has not been optimized based on bone quality [10].

Bone quality, which has been defined as "the sum of all characteristics of bone that influence the bone's resistance to fracture [11]", is completely independent of bone mineral density (BMD), and many clinical studies have indicated that increases in BMD following treatment with *anti*-resorptive drugs do not reflect a proportional reduction in relative fracture risk [12], which suggests that bone quality plays an essential role in determining bone strength [13]. In a consensus statement issued by the National Institutes of Health (NIH), bone quality was defined more concretely as bone architecture, bone turnover, bone mineralization and micro-damage accumulation [13]. In implant dentistry, however, bone quality is still considered equivalent to bone density on radiographic assessments [14,15]. Although the paradigm of bone quality has shifted from density-based assessments to structural evaluations of bone, clarifying bone quality based on structural bone evaluations remains challenging in implant dentistry because devices capable of accurately evaluating bone structure have yet to be developed.

In our previous studies, the preferential orientation of biological apatite (BAp) crystal and collagen fibers (hereafter BAp *c*-axis/collagen fibers) was proposed as a new index for assessing bone quality [16–19]. BAp, which is one of the main inorganic components of hard tissue, crystallizes on the type-I collagen, which is a main organic component, so that the BAp *c*-axis is almost parallel with the direction of the collagen fibers [20]. Preferential orientation refers to nano-scale anisotropic organization in a vector form (consisting of the direction and magnitude of bone tissue), which is not adequately described by the BMD as a scalar parameter. Regardless of BMD, bone shows a wide variety of orientation distribution depending on type and anatomical location [16], which results in its anisotropic mechanical performance. Therefore, BMD alone cannot be used to fully evaluate the mechanical properties of bone. A combination of BMD and preferential orientation might be highly beneficial in the assessment of bone function.

In the fields of dentistry and implant dentistry, the mandible bone is a primary focus. In our previous studies, the preferential orientation degree of BAp *c*-axis/collagen fibers was applied to evaluate mandible function and the development of dental implants [17,19]. Similar to the long bone, which shows unidirectional orientation along the longitudinal axis [16], the mandible basically shows uni-directional orientation of BAp along the mesiodistal axis; however, the direction of maximum orientation was initially reported to change locally to the biting direction just beneath the teeth [16]. This suggests that mechanical load alters anisotropy in the microstructural arrangement of bone and affects

other mechanical properties. Therefore, BAp and collagen orientation are highly important in the development of dental implants because they directly transfer mechanical load to the host bone tissue through mastication.

In addition, osteocytes are known to play a substantial role in modifying the macro- and microstructures of bone based on mechanosensation and mechanotransduction [21,22], even though the way in which osteocytes regulate bone structure remains a matter of debate. Nonetheless, focusing on osteocytes in an attempt to understand alterations in bone quality around dental implants seems worthwhile.

The aims of the present study were to investigate the effect of implant neck groove designs on bone quality under controlled repetitive mechanical loading and to determine the optimal implant design by evaluating bone microarchitecture around implants using light microscopy, polarized light microscopy, and a microbeam X-ray diffractometer (μXRD).

2. Materials and methods

2.1. Implant neck designs

Anodized Ti-6Al-4V alloy dental implants with three grooves around the neck were used (3.7 × 6.0 mm; Kyocera Co. Ltd., Kyoto, Japan). On the implants, +60° and −60° grooves, defined as 60° downward and upward directions to a plane perpendicular to the long axis, respectively, were introduced by machining (Kyocera Co. Ltd., Kyocera, Japan) (n = 14 each). The pitch and depth of the grooves were 400 μm and 200 μm, respectively (Fig. 1a).

2.2. Implant placement

Fourteen adult Japanese white rabbits (mean weight: 3.85 ± 0.24 kg) were obtained for use in this study (Biotek Co. Ltd., Saga, Japan). First, 56 Ti-6Al-4V screws (Kyocera Co. Ltd.) were used to anchor a custom-made loading device (Higuchi Co. Ltd., Nagasaki, Japan). The implants with −60° grooves were placed in the tibial metaphysis of a randomly selected side of each rabbit, and the implants with +60° grooves were placed in the other side. Two anchor screws were placed in both sides of the implant 2 mm from the implant surface. Implant placement was performed unicortically under a combination of local and general anesthesia (35 mg/kg ketamine and 5 mg/kg xylazine, respectively). The study protocol was approved by the Ethics Committee for Animal Research of Nagasaki University, and animals were treated in accordance with the guidelines for Animal Experimentation of Nagasaki University.

2.3. Loading protocol

All implants received healing abutments at 12 weeks after implant placement. The 14 rabbits were then randomly divided into two groups. In an experimental group (n = 7), both implants in each rabbit were subjected to a cyclic mechanical load in accordance with that used in our previous study [19]. Briefly, the implants were subjected to a mechanical load of 50 N with a frequency of 3 Hz for 1800 cycles which is equivalent to chewing and swallowing cycles in humans [23], 2 days/week for 8 weeks using a loading device supported by two lateral screws on each implant under general anesthesia. The load direction was parallel with the long axis of the implants. The rabbits in the other group (n = 7) served as controls and were not subjected to a mechanical load (Fig. 1b).
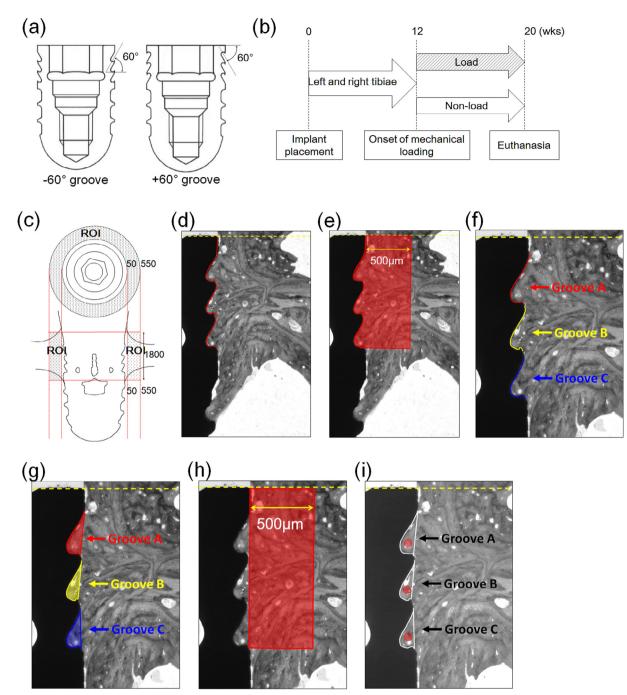
Fig. 1. (a) The implant designs used in this study; (b) Twelve weeks after implant placement, repetitive mechanical loading (50 N with a frequency of 3 Hz for 1800 cycles, 2 days/week) was applied to implants with −60° and +60° grooves placed in randomly selected rabbits (7 rabbits, 14 implants) for 8 weeks. The remaining rabbits were used as controls (7 rabbits, 14 implants); (c) The region of interest (ROI) on microcomputed tomography (microCT) analysis was established at a range of 50–550 μm away from the implant surface and 1800 μm downward from the top of the implant; (d) The red line indicates the length of the implant from the implant neck to the inferior border of the lower grooves for the assessment of bone-implant contact (BIC) (the yellow dashed line indicates the top of the implant); (e) The red area was used for the evaluation of bone area fraction (BAF) (two-headed arrow: 500 μm; the dashed line indicates the top of the implant); (f) The grooves were designated as grooves A, B, and C sequentially from the implant top; (g) The colored areas show where osteocyte density and the alignment of collagen fibers were measured inside area of grooves (red, yellow, and blue areas indicate grooves A, B, and C, respectively); (h) The red areas show where osteocyte density and the alignment of collagen fibers were measured in outside groove area (two-headed arrow: 500 μm); (i) The red circles show the areas of interest (AOI) for the measurement of the orientation direction of the BAp c-axis (100-μm diameter within each groove). (For interpretation of the references to colour in this figure legend, the reader is referred to the web version of this article.)

2.4. Microcomputed tomography (microCT) assessment

All rabbits were sacrificed at 8 weeks after the initiation of a mechanical load. Tibia blocks with implants and anchor screws were then cut using a diamond saw (Exakt®; Heraeus Kulzer GmbH, Hanau, Germany). After fixation in 10% neutral buffered formalin for 48 h, the tibia blocks were scanned using microCT at 20-μm voxel resolution and 90-kV tube voltage (R_mCT2, Rigaku Co. Ltd., Tokyo, Japan). Bone around the implant in the proximal tibial metaphysis was segmented and reconstructed using a semi-manual contouring method with TRI/3D-BON (Ratoc System Engineering, Tokyo, Japan) [24]. The region of interest (ROI) was

established at a range of 50–550 μm away from the implant surface and 1800 μm downward from the top of the implant in order to avoid metal artifacts [25]. The extracortical bone area above the implant was excluded from the ROI (Fig. 1c). Digital images were analyzed using TRI/3D-BON. Bone volume fraction [BVF (%) = bone volume in ROI/tissue volume in ROI], trabecular number (Tb.N), trabecular thickness (Tb.Th), trabecular separation (Tb.Sp), and BMD were then semi-automatically measured in accordance with the guidelines for assessment of bone microstructure using microCT [26].

2.5. Histology

The tibial bone blocks were then dehydrated in ethanol and embedded in methyl methacrylate resin (methyl methacrylate polymer and monomer [Wako Pure Chemical Industries, Ltd., Osaka, Japan]). Resin-embedded samples were cut longitudinally to include the implant and anchor screws using a diamond saw (Exakt; Heraeus Kulzer GmbH, Hanau, Germany). The specimens were then ground to approximately 15-μm thickness and stained with toluidine blue. The bone around the implant neck was then histomorphometrically assessed to detect the following: 1) bone-to-implant contact (BIC); 2) bone area fraction (BAF); and 3) number of osteocytes (osteocyte density). Each area of interest (AOI) was defined as follows: 1) BIC (%) = the length of bone to implant contact from the top of the implant to the inferior border of the lower grooves (mm)/the length from the implant neck to the inferior border of the lower grooves (mm) × 100 (Fig. 1d); and 2) BAF (%) = total bone area ranging from 0 to 500 μm away from the implant surface (mm^2) and from the top of the implant to the inferior border of the lower grooves / total tissue area ranging from 0 to 500 μm away from the implant surface (mm^2) and from the top of the implant to the inferior border of the lower grooves × 100 (Fig. 1e); and 3) osteocyte density (#/mm^2) = number of osteocytes (#) in total bone area from 0 to 500 μm away from the implant surface (mm^2) and from the top of the implant to the inferior border of the lower grooves (Fig. 1e). The AOI did not include the extracortical bone above the implant neck.

2.6. Evaluation of bone quality inside and outside each groove area; osteocyte density, and preferential orientation degree of BAp c-axis/collagen fibers in grooves A, B, and C

Osteocyte density and the orientation degree of BAp c-axis/collagen fibers were investigated to evaluate bone quality based on bone microarchitecture inside and outside each groove area. The grooves were sequentially designated from the top of the implant as grooves A, B, and C, respectively (Fig. 1f). Osteocytes in osteocyte lacunae were detectable in resin-embedded toluidine blue-stained samples under high magnification using light microscopy (BZ-9000; Keyence, Osaka, Japan) [27,28]. The number of osteocytes inside and outside each groove area were then counted (the AOIs for the inside and outside areas are shown in Fig. 1g and h, respectively). To assess the alignment of collagen fibers inside and outside each groove area, polarized light microscopy (Optiphot-2 Pol, Nikon Corporation, Tokyo, Japan) with the polarizer and analyzer in the cross position was used, as previously described (AOIs for the inside and outside areas are shown in Fig. 1g and h, respectively) [19]. Briefly, in order to analyze the direction of maximum collagen orientation, the sectioned specimens were rotated under polarized light microscopy to find the rotation angle associated with the brightest AOI region. The brightness of each AOI was determined using NIH Image-J version 1.47, and the angles for the preferential orientation of collagen fibers for the groove direction were determined, with the counterclockwise angle defined as positive. To quantitatively analyze the direction of preferential BAp orientation more precisely, a μXRD with a transmission optical system (R-Axis BQ; Rigaku Co. Ltd., Kyoto, Japan), which has been shown to have high quantitativeness in analyzing particularly crystalline inorganic materials, was used as previously reported [29]. Briefly, Mo-Kα radiation was generated at 50 kV and 90 mA. The incident beam was collimated into a 100-μm circular spot using a double-pinhole metal collimator, and was projected vertically onto the specimen to analyze the two-dimensional (2D) distribution of BAp c-axis alignment along the surface of the specimens (Fig. 1i). The diffracted beam was collected for 3600 s. From the obtained Debye ring, the diffracted intensities from the (0 0 2) and (3 1 0) BAp planes were integrated along the azimuthal angle (β) at steps of 1°. Intensity distributions of the (0 0 2) and (3 1 0) as a function of β(I(β)) were approximated by the following modified-elliptic polynomial function using the least-squares method [29]:

$$I(\beta) = \left\{ \frac{cos^2(\beta - \mu)}{a^2} - \frac{sin^2(\beta - \mu)}{b^2} \right\}^{\frac{1}{2}} - c$$

where a, b, c, and μ are the fitting parameters and μ is the angle at which the intensity peaks. Finally, the degree of BAp c-axis alignment was calculated as the intensity ratio of (0 0 2)/(3 1 0) for each β, resulting in 2D BAp c-axis alignment along the plane vertical to the incident X-ray beam. The 2D distribution of BAp alignment was expressed as a radar diagram. Finally, angles were determined for preferential BAp c-axis alignment from the groove direction.

2.7. Statistical analyses

All statistical analyses were performed blindly. The Shapiro-Wilk test was performed for normality. The paired t test was used to compare the −60° and +60° groove implants in both non-loaded and loaded conditions, and the independent t test was used to compare the non-loaded and loaded conditions. Sample size was determined by power calculations to obtain 80% statistical power by referring to a previous study [27]. All statistical analyses were conducted using Systat 12 (Systat Software, Chicago, IL). An α-level of 0.05 was considered to indicate statistical significance. All data are represented as the mean ± SEM.

3. Results

3.1. Effect of neck design on bone quantity and quality without mechanical loading

No infection was observed on representative images of toluidine blue-stained sections (Fig. 2a). Both BIC and BAF around the implant neck were similar, irrespective of groove design (Fig. 2b and c, respectively). The osteocyte densities in bone around the dental implants with +60° and −60° grooves were similar (Fig. 2d). Regarding angle differences between the groove direction and collagen alignment (Fig. 2e), smaller values indicate more parallel collagen alignment with the groove direction. The collagen alignment was almost parallel to the groove direction, which deviated less than 10° in both +60° and −60° grooves.

3.2. Effect of mechanical loads on osseointegration, bone quantity, and bone quality in implants with −60° and +60° grooves

Bone healing occurred normally without any infection based on representative images of toluidine blue-stained sections with mechanical loading (Fig. 3a). A higher degree of BIC was noted in +60° grooves with mechanical loading, whereas a trend of superior BIC, even in −60° grooves was noted with mechanical loading (Fig. 3b). The BAF around implant necks was significantly increased
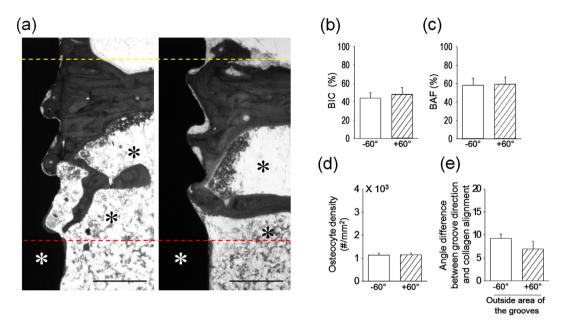
Fig. 2. Effect of groove designs on bone around dental implants without mechanical loading. (a) Representative images of toluidine blue-stained sections (yellow dashed line: implant top; red dashed line: inferior border of the lower groove; black asterisk: bone marrow; white asterisk: implant). Bar = 500 µm; (b) BIC was similar, regardless of groove design; (c) BAF was nearly identical between −60° and +60° grooves without mechanical loading; (d) Osteocyte density was the same without mechanical loading, regardless of groove design; (e) Angle differences between groove direction and collagen alignment were the same between −60° and +60° grooves without mechanical loading. n = 7 per group. (For interpretation of the references to colour in this figure legend, the reader is referred to the web version of this article.)

with mechanical loading, regardless of groove design (Fig. 3c). Total osteocyte density in +60° grooves was significantly increased with mechanical loading, but that in −60° grooves was similar due to mechanical load (Fig. 3d). Moreover, osteocyte density inside and outside each +60° groove area was significantly increased with mechanical loading, but no significant change was observed in −60° groove areas, regardless of mechanical load (Fig. 3e and f, respectively). The angle differences between the groove direction and collagen alignment outside grooves were significantly larger in the mechanical load group than in the control group, regardless of groove design (Fig. 3g).

3.3. Effect of groove designs on bone structure and BMD around the implant neck with mechanical loading

MicroCT was conducted to clarify the effect of groove design on bone microstructure around the implant neck with mechanical loading. Representative images of microCT are shown in Fig. 4a. BVF around the necks with +60° grooves was significantly higher than that around the necks with −60° grooves with mechanical loading (Fig. 4b). A trend of more Tb.N was observed around the necks with +60° compared with the necks with −60° grooves ($p = 0.052$) (Fig. 4c). Tb.Th for the necks with −60° grooves was almost same as that for necks with +60° grooves (Fig. 4d), whereas Tb.Sp around the necks with +60° grooves was significantly decreased compared with that of necks with −60° grooves (Fig. 4e). No differences were observed in BMD among implants, regardless of groove design (Fig. 4f).

3.4. Effect of groove designs on bone quality defined as osteocyte numbers and orientation degree of the BAp c-axis/collagen fibers in the inside areas of both types of grooves with mechanical loading

To clarify the effects of groove design on bone quality around the implant necks with +60° and −60° grooves, the orientation degree of the BAp c-axis/collagen fibers were investigated for each type of groove (A, B, and C). Representative images obtained from

polarized light microscopy are shown in Fig. 5a. The angle differences between groove direction and the alignment of collagen fibers were evaluated. In groove B, the angle differences in +60° grooves were significantly smaller than those in −60° grooves. In groove A, the differences in +60° grooves were also smaller than those in −60° grooves, although these differences were not statistically significant. No differences were observed between +60° and −60° grooves in groove C (Fig. 5b). In order to more precisely quantify the preferentially aligned direction of extracellular matrix, the 2D distribution of BAp c-axis alignment was analyzed in the plane containing the groove direction. Representative toluidine blue-stained images and radar diagrams inside each groove are shown in Fig. 6a. The direction of the major axis of the modified ellipse corresponds to the direction of the preferential BAp c-axis alignment. The BAp alignment direction is summarized in Fig. 6b. The BAp c-axis alignment with the grooves in grooves A and B was approximately parallel, as indicated by the small angle difference. On the other hand, in groove C, the angle differences were scattered (relatively large SEM) in both grooves. The directionalities of the BAp c-axis and collagen showed similar trends in all grooves, which can clearly be seen when comparing Fig. 5 and Fig. 6b.

3.5. Schematics of the preferential alignment of the BAp c-axis and collagen around the implant grooves

The preferential alignment of the BAp c-axis and collagen in the bone tissue inside and around the implant grooves is illustrated in Fig. 7a and b. The directions of the BAp c-axis/collagen fibers were identical according to the present results (Fig. 5b and Fig. 6b). The results for groove C were not adopted because of unexpected stress condition (see Discussion). For the implant with −60° grooves, the BAp c-axis/collagen fibers in the groove somewhat aligned along the groove wall (Fig. 5b and Fig. 6b); outside the groove, these aligned near parallel to the implant axis (about 20° anticlockwise from the −60° groove direction, as shown in Fig. 3g). For the implant with +60° grooves, the BAp c-axis/collagen fibers in the groove aligned well along the groove (Fig. 5 and Fig. 6b); outside
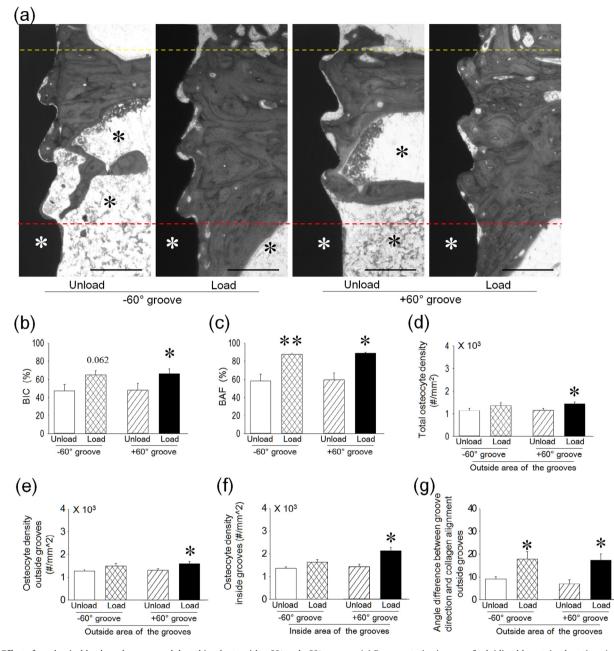
Fig. 3. Effect of mechanical loads on bone around dental implants with −60° and +60° grooves. (a) Representative images of toluidine blue-stained sections (yellow dashed line: implant top; red dashed line: inferior border of the lower groove; black asterisk: bone marrow; white asterisk: implant). Bar = 500 µm; (b) BIC for +60° grooves was significantly increased with mechanical loading, while a trend of more BIC for −60° grooves was noted; (c) BAF was significantly increased with mechanical loading, irrespective of groove design; (d) Total osteocyte density in +60° grooves was significantly increased with mechanical loading, but that in −60° grooves was nearly the same, regardless of mechanical load; (e) The application of a mechanical load significantly increased osteocyte density inside the groove area of +60° grooves, but not of −60° grooves; (f) Osteocyte density outside the groove area of the +60° grooves was significantly greater with mechanical loading, whereas no change was seen in −60° grooves, irrespective of mechanical load; (g) The application of a mechanical load resulted in significant changes in angle differences between groove direction and collagen alignment, regardless of groove design. n = 7 per group, $^*p < 0.05$ vs unload group, $^{**}p < 0.01$ vs unload group. (For interpretation of the references to colour in this figure legend, the reader is referred to the web version of this article.)

the groove, these aligned obliquely downward to the host bone (Fig. 3g). In the host long bone portion sufficiently distant from the implant, BAp c-axis/collagen fibers preferentially aligned along the bone longitudinal axis.

Therefore, a significant difference in the stress transfer was suggested between the implants with −60° and +60° grooves, resulting in optimal stress transfer from the implant under the applied load to the host bone via the new bone inside +60° grooves, and the subsequent preferential alignment of the BAp c-axis/collagen fibers for the implant with +60° grooves, as shown in Fig. 7a and b.

4. Discussion

The results of this study demonstrated that implant neck design substantially affects bone quality, defined as the preferential alignment of BAp c-axis/collagen fibers and osteocytes around dental implants. Designed implants with +60° grooves may be optimized so that biting stress is effectively transmitted to the host bone, similar to the natural tooth-mandible system. Teeth with a tapered shape, effectively transmit biting stress to the mandible alveolar bone in an obliquely downward direction [30–32]. As a result, in
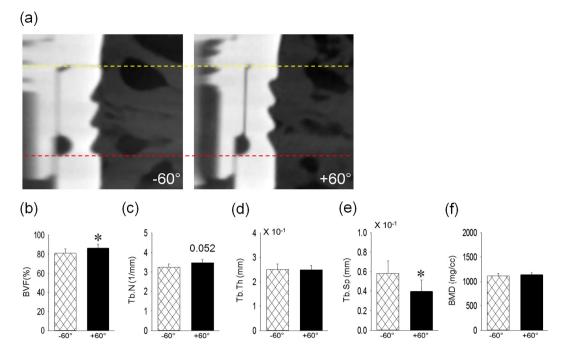
Fig. 4. MicroCT evaluation. (a) Representative images of microCT-scanned sections (yellow dashed line: implant top; red dashed line: inferior border of the lower groove; (b) Bone volume fraction in +60° grooves was significantly increased compared with that in −60° grooves; (c) A trend of more trabecular number was noted in +60° grooves; (d) Trabecular thickness was also similar among −60° and +60° grooves; (e) Trabecular separation in +60° grooves was significantly smaller than that in −60° grooves; (f) BMD was almost the same with mechanical loading, regardless of groove design. n = 7 per group, $^*p < 0.05$. (For interpretation of the references to colour in this figure legend, the reader is referred to the web version of this article.)

our previous study, the BAp c-axis has been shown to orient locally in a biting-related direction near the tooth, while the mandible basically shows uni-directional BAp c-axis orientation along the mesiodistal axis [16]. In this study, the implants with +60° grooves formed the preferential orientation of BAp c-axis/collagen along the obliquely downward direction, which is a condition similar to the original tooth-mandible system. This indicates that a stress distribution similar to the original condition was achieved because the direction of BAp c-axis/collagen orientation mirrors the direction of principal stress *in vivo* [14,26]. Our previous study using beagle dogs also demonstrated that +60° grooves on a metallic hip implant that elongated in the direction of the original stress transmission generated principal stress parallel to the groove direction when the implant was loaded; however, −60°, −30°, 0°, and +30° grooves on hip implants did not effectively transfer principal stress to the direction of each groove angle [29]. Moreover, stress concentration mainly occurs in the neck of osseointegrated dental implants [2]. Based on these three perspectives, −60° and +60°, but not −30°, 0°, and + 30° grooves, were applied to the neck design of dental implants in the current study. Indeed, the BAp c-axis/collagen fibers became preferentially orientated in the groove direction in the +60° groove with mechanical loading. Stress was continuously transmitted to the host bone (the tibia), which was demonstrated by the rotation of the BAp/collagen oriented direction as a function of the distance from the implant. By the contrast, in the −60° groove, the BAp and collagen tended to misalign from the groove direction. Without mechanical loading, the groove angle did not affect bone quality, which further emphasizes the importance of mechanical stimuli for the maintenance of bone quality.

In the +60° groove, the alignment of bone BAp and collagen in groove C differed and scattered compared with grooves A and B with mechanical loading (Fig. 5b and Fig. 6b). Groove C was located below the cortices of the host tibia; therefore, optimal stress transmission may not have been achieved because less bone was pre-

sent in the obliquely downward area, which plays a primary role in transmitting stress to the host bone. The location of grooves on the implant neck should be carefully considered to improve bone quality parameters around dental implants.

Osteocytes are believed to be mechanosensors in the bone matrix [33]. It has been reported that the number of osteocytes increase after natural or artificial loading [19,34–36]. The osteocyte population seems to increase in response to an increase in external mechanical requirements. In this study, osteocyte density both inside and outside the +60° groove significantly increased with mechanical loading. This supports the hypothesis that the load applied to the implant was successfully transmitted to the bone tissue inside the +60° groove and around the implant.

In the current study, load conditions were applied in accordance with our previous studies using a custom-made loading device that controls load amplitude, frequency, cycle and duration [19,34]. Bone gain in response to the application of a mechanical load has been considered to depend on strain magnitude. According to Frost's mechanostat theory, bone formation occurs when the strain magnitude ranges from 1500 to 3000 µstrain [37,38]. In this study, preliminary data using cadaver samples were in the range of the theory that induces bone formation (data not shown), which suggests that predetermined load amplitude and frequency may have an anabolic effect around dental implants in response to the application of a mechanical load. Indeed, in this study, mechanical loads significantly increased BAF around the implants, regardless of groove design.

Tooth contact occurs in 1800 cycles/day during chewing and swallowing in humans [23]. A recent *in vitro* study reported that the proliferation rate of human osteoblasts was highest by continuous mechanical stimuli at 1800 cycles/day [39]. It has also been demonstrated that the rapid promotion of *c-fos* gene expression of human osteoblasts is induced by mechanical loading at 1800 cycles for 30 min [40]. Therefore, 1800 cycles/day was determined to activate bone cells in the present study. On the other hand, an
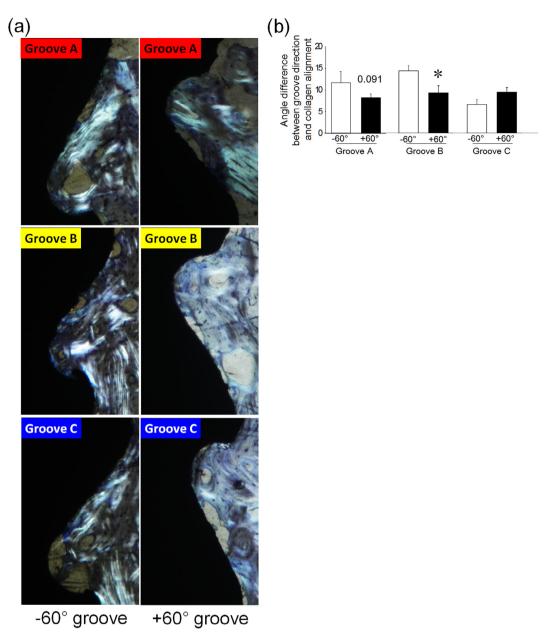
Fig. 5. Effect of mechanical loads on preferential alignment of collagen fibers in each groove. (a) Representative images obtained from polarized light microscopy; (b) The angle difference between groove direction and alignment direction of collagen fibers in +60° groove B was significantly smaller than that in −60° groove B. A trend of smaller angle differences between groove direction and collagen alignment in +60° groove A was observed, but these differences did not change between groove designs in groove C. n = 7 per group, *$p < 0.05$.

in vivo study showed that bone mineral contents were not altered by the load cycle numbers from 36 to 1800 cycles/day with the same load frequency and amplitude [41]. Although the load cycle of 1800 markedly affected bone quantity and quality around dental implants in the present study, further studies are needed to clarify the effect of load cycle number on bone around dental implants.

The natural chewing frequency of New Zealand white rabbits is between 3.3 Hz to 4.0 Hz [42,43], and tibial bone volume is similar to that of mandible [44]. With regard to the anisotropic micro-organization, tibial bone and mandible show identical preferential orientation in the uni-directional orientation of BAp *c*-axis/collagen fibers in the longitudinal and mesiodistal axis, respectively [16]. Thus, from the perspectives of size and microstructure, tibia bone seems to be useful in research involving dental implants. Moreover, the intraoral application of a custom loading device is challenging. Therefore, in this study, rabbit tibiae were used

instead of jaw bone at a loading frequency of 3.0 Hz. However, long and jaw bone marrow have recently been shown to have different osteoclastogenic potential in mice, meaning that the response to the application of a mechanical load around implants in long bone might be different from that in jaw bone. More data are needed to clarify the effects of controlled mechanical loads around dental implants in jaw bone. In this study, the net effect of implant designs and mechanical loads on bone around dental implants placed in rabbit tibiae was investigated. Complete bone healing requires 8–12 weeks after surgery in rabbit tibiae [45,46]. Hence, to avoid any synergic effects due to the bone wound healing process, no mechanical load was applied until 12 weeks after the placement of implants.

The differences in implant neck design are associated with different mechanical characteristics on the bone around dental implants. In an animal study, a significantly higher degree of BIC
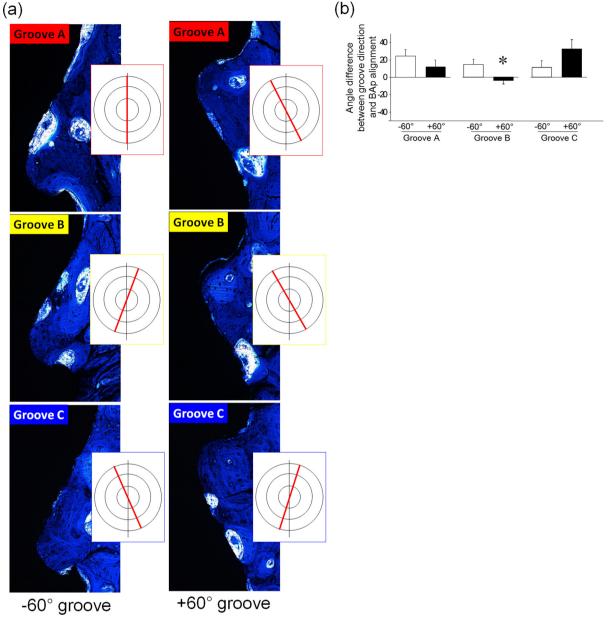
Fig. 6. Effect of mechanical loads on preferential alignment of the BAp c-axis in each groove. (a) Representative images of toluidine blue-stained images and radar diagrams of preferential alignment of the BAp c-axis; (b) Angle differences between groove direction and BAp c-axis alignment in +60° groove B was significantly smaller than that in −60° groove B, while no differences were noted in +60° groove C and −60° groove C. In groove A, the differences were similar, regardless of groove design. n = 7 per group, *p < 0.05. (For interpretation of the references to colour in this figure legend, the reader is referred to the web version of this article.)

was reported for Astra Tech implants with microthreads on the neck (AstraTech AB, Mölndal, Sweden) than for implants without microthreads [5]. In a prospective clinical study, the marginal bone level around implants both with and without microthreaded necks has been stable for 3 years; however, different patterns of marginal bone resorption has been observed between these two implant designs [9]. Moreover, the groove profile of implants plays an important role in establishing early osseointegration, maintaining marginal bone level, and acquiring implant stability. Previous studies that conducted a finite element analysis [47] and an animal experiment [48] discussed important aspects in relation to the effects of thread shape. In a rabbit study, square threaded implants had a significantly higher degree of BIC and greater removal torque than V-shape and reverse buttress threaded implants [48]. In an another rabbit study, implants with grooves having pitches of either 110 or 200 μm and a depth of 70 μm at the thread flank

showed significantly higher removal torque and affinity for bone formation than control implants [49]. Moreover, grooves having a pitch of 110 μm and a depth of 70 μm on the center of the inferior thread flank (Brånemark systems MK III Groovy, Nobel Biocare AB) have been shown to facilitate more rapid bone integration and to improve implant stability [50]. Although bone quality was not investigated in those animal studies, the findings suggested that implants with these groove sizes and shapes might optimize bone quantity. An earlier study reported that the recommended minimum pore size for a scaffold was 100 μm [51]. However, recent studies have demonstrated that a pore size of more than 300 μm is required to obtain more vascularization, oxygenation, and enhanced cell migration to promote bone formation, whereas a pore size smaller than 120 μm induces fibrous tissue and/or chondrogenesis before osteogenesis [52–56]. On the other hand, pore size does have an upper limit, because the mechanical properties
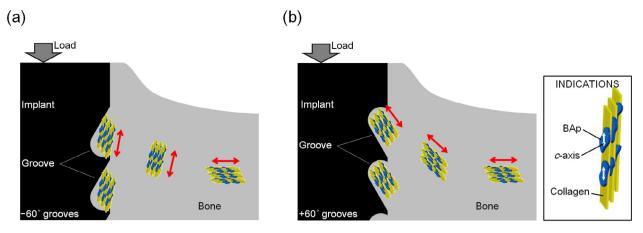
Fig. 7. Schematics of the preferentially aligned bone microstructure of BAp *c*-axis/collagen fibers in the case that the groove angle was (a) −60° and (b) +60°, reproduced based on the data in Fig. 3g, Fig. 5b, and Fig. 6b. Only in the +60° groove, the direction of the BAp *c*-axis/collagen fiber alignment continuously changed from inside of the groove to the host tibia bone through the bone inside the groove.

of the implant materials are attenuated by overly large pore sizes. Therefore, in this study, the pitch and depth of grooves for newly developed implants were designed to be 400 μm and 200 μm, respectively. Interestingly, the groove designs did not affect bone quantity when no mechanical load was applied, and the differences in neck design did affect bone quantity around both types of implants with mechanical loading. The application of a mechanical load significantly increased BIC and bone volume with more Tb.N and less Tb.Sp in bone around +60° grooves than in bone around −60° grooves. These findings indicate that bone wound healing around implants is similar without mechanical loading, even if the neck design is different; however, if a mechanical load is applied, implants with +60° grooves are superior to those with −60° grooves in terms of bone quantity around implants.

In this study, bone quality was considered as "the sum of all characteristics of bone that influence the bone's resistance to fracture [11]". However, in implant dentistry, bone quality is based on radiographic assessments such as the proportion of cortical and trabecular bone in jaw bone [14] and/or Hounsfield units [15], thus directly reflecting BMD. Importantly, "bone quality" is completely independent of BMD, meaning that a complete explanation of bone mechanical function needs to account for not only BMD, but also bone quality. Indeed, bone strength has been thought to consist of BMD (70%) and bone quality (30%) [13]. However, this present study focused on osteocyte density and the BAp *c*-axis/collagen fibers in order to account for bone mechanical function around implants. The application of a mechanical load significantly increased BMD, regardless of groove design (data not shown), suggesting that repetitive mechanical loads partially improved bone strength in both types of implants. The differences in groove design did not affect bone quality defined as osteocyte density and the preferential alignment of collagen fibers without mechanical loading, whereas the differences in groove angles markedly influenced bone quality with mechanical loading. The application of a mechanical load significantly increased osteocyte density in bone around implants with +60° grooves; however, unexpectedly, it did not affect the osteocyte density in bone around −60° grooves. Recently, it was demonstrated that cyclic mechanical loads significantly increase osteocyte density around implants without grooves based on light microscopy and scanning electron microscopy [19,34]. Other clinical studies in humans have also shown that the application of a mechanical load significantly increases the number of osteocytes around dental implants in jaw bone [35,36]. The present findings suggest that the increase of BMD and osteocytes does not necessarily occur simultaneously,

although both responses are commonly found in the loaded bone. The directionality and magnitude of stress applied to the bone in −60° and +60° grooves may conflict with one another, which is one possible reason for the differences in the alteration behavior of BMD and osteocyte density. Furthermore, it is possible that a stress threshold activates the alteration of BAp and collagen alignment, independent of that responsible for changes in BMD and osteocyte density. Further studies should be performed to clarify the stress threshold in bone responsible for the alteration of each index.

The establishment of continuous directionality of the preferential orientation of BAp *c*-axis/collagen observed around +60° grooves indicated a continuous stress distribution within the bone because the BAp *c*-axis/collagen orientation direction reflects principal stress *in vivo* [26]. The application of optimal stress to the peripheral bone is an essential factor in the long-term stability of implants [57].

As a result of the establishment of the aligned microstructure of BAp and collagen, the enhancement of mechanical integrity is highly expected. Our previous study clarified that the degree of BAp *c*-axis alignment, rather than BMD, controls Young's modulus which is one of the most important parameters for showing the mechanical performance of bone [58]. Moreover, osteocyte density was shown to be necessary to maintain and modify bone mass along with applied mechanical conditions [59]; the increased osteocyte density demonstrated in the present study may contribute to the long-term maintenance of bone in this specific condition. These new findings are therefore expected to provide a novel indication for the design and development of implant devices and to improve the mechanical function of bone and the mechanical stability of implants after the application of mechanical loading. Long-term implantation studies and mechanical analyses such as the torque test or pull-out test should be conducted to further reveal the clinical effectiveness of grooved dental implants.

5. Conclusion

In this study, the effectiveness of newly designed dental implants with +60° groove structures in the neck was clearly demonstrated. The direction of the preferential orientation of BAp *c*-axis/collagen around the +60° grooves continuously changed from inside of the groove to host bone when loaded. Stress application was important for establishing the preferentially aligned microstructure of BAp *c*-axis/collagen fibers that dominates the

mechanical properties of bone, and upregulation of osteocyte density was associated with mechanosensing. Bone quality around dental implants, as well as BMD, could become a new clinical parameter to account for bone strength in implant dentistry. The present findings are expected to provide a novel indication for the design and development of implant devices that realize the enhanced mechanical function of surrounding bone and the long-term stability of such devices.

Disclosures

The authors declare that there are no conflicts of interest.

Acknowledgements

References

[1] T. Albrektsson, G. Zarb, P. Worthington, A.R. Eriksson, The long-term efficacy of currently used dental implants: a review and proposed criteria of success, Int. J. Oral Maxillofac. Implants 1 (1986) 11–25.

[2] M.I. Hudieb, N. Wakabayashi, S. Kasugai, Magnitude and direction of mechanical stress at the osseointegrated interface of the microthread implant, J. Periodontol. 82 (2011) 1061–1070.

[3] R. Amid, S. Raoofi, M. Kadkhodazadeh, M.R. Movahhedi, M. Khademi, Effect of microthread design of dental implants on stress and strain patterns: a three-dimensional finite element analysis, Biomed. Technol. (Berl) 58 (2013) 457–467.

[4] I. Ericsson, C.B. Johansson, H. Bystedt, M.R. Norton, A histomorphometric evaluation of bone-to-implant contact on machine-prepared and roughened titanium dental implants. A pilot study in the dog, Clin. Oral Implants Res. 5 (1994) 202–206.

[5] I. Abrahamsson, T. Berglundh, Tissue characteristics at microthreaded implants: an experimental study in dogs, Clin. Implant Dent. Relat. Res. 8 (2006) 107–113.

[6] D.L. Cochran, R.K. Schenk, A. Lussi, F.L. Higginbottom, D. Buser, Bone response to unloaded and loaded titanium implants with a sandblasted and acid-etched surface: a histometric study in the canine mandible, J. Biomed. Mater. Res. 40 (1998) 1–11.

[7] L.J. Heitz-Mayfield, B. Schmid, C. Weigel, S. Gerber, D.D. Bosshardt, J. Jönsson, N.P. Lang, Does excessive occlusal load affect osseointegration? An experimental study in the dog, Clin. Oral Implants Res. 15 (2004) 259–268.

[8] Y. Miyamoto, K. Koretake, M. Hirata, T. Kubo, Y. Akagawa, Influence of static overload on the bony interface around implants in dogs, Int. J. Prosthodont. 21 (2008) 437–444.

[9] D.W. Lee, Y.S. Choi, K.H. Park, C.S. Kim, I.S. Moon, Effect of microthread on the maintenance of marginal bone level: a 3-year prospective study, Clin. Oral Implants Res. 18 (4) (2007) 465–470.

[10] H.M. Alharbi, N. Babay, H. Alzoman, S. Basudan, S. Anil, J.A. Jansen, Bone morphology changes around two types of bone-level implants installed in fresh extraction sockets–a histomorphometric study in Beagle dogs, Clin. Oral Implants Res. 26 (9) (2015) 1106–1112.

[11] D.P. Fyhrie, Summary-measuring "bone quality", J. Musculoskelet. Neuronal Interact. 5 (2005) 318–320.

[12] R. Pauwels, R. Jacobs, S.R. Singer, M. Mupparapu, CBCT-based bone quality assessment: are Hounsfield units applicable?, Dentomaxillofac Radiol 44 (2015) 20140238

[13] NIH consensus development panel on osteoporosis prevention, and therapy, osteoporosis prevention, diagnosis, and therapy, JAMA 285 (2001) 785–795.

[14] U. Lekholm., G. Zarb., Patient Selection and Preparation. In: Tissue-Integrated Prostheses, Osseointegration in Clinical Dentistry (eds P.-I. Branemark, G. Zarb. & T. Alnreltsson), Quintessence, Chicago, IL, 1985, pp. 199–210.

[15] C. Misch, Contemporary Implant Dentistry, second ed., Mosby, St Louis, MO, 1999.

[16] T. Nakano, K. Kaibara, Y. Tabata, N. Nagata, S. Enomoto, E. Marukawa, Y. Umakoshi, Unique alignment and texture of biological apatite crystallites in typical calcified tissues analyzed by microbeam X-ray diffractometer system, Bone 31 (2002) 479–487.

[17] T. Morioka, S. Matsunaga, M. Yoshinari, Y. Ide, T. Nakano, H. Sekine, Y. Yajima, Alignment of biological apatite crystallites at first molar in human mandible cortical bone, Cranio 30 (2012) 32–40.

[18] T. Nakano, K. Kaibara, T. Ishimoto, Y. Tabata, Y. Umakoshi, Biological apatite (BAp) crystallographic orientation and texture as a new index for assessing the microstructure and function of bone regenerated by tissue engineering, Bone 51 (2012) 741–747.

[19] S. Kuroshima, M. Yasutake, K. Tsuiki, T. Nakano, T. Sawase, Structural and qualitative bone remodeling around repetitive loaded implants in rabbits, Clin. Implant Dent. Relat. Res. 17 (2015) e699–e710.

[20] W.J. Landis, The strength of a calcified tissue depends in part on the molecular structure and organization of its constituent mineral crystals in their organic matrix, Bone 16 (1995) 533–544.

[21] J. Klein-Nulend, R.G. Bacabac, A.D. Bakker, Mechanical loading and how it affects bone cells: the role of the osteocyte cytoskeleton in maintaining our skeleton, Eur. Cell Mater. 24 (2012) 278–291.

[22] J. Klein-Nulend, A.D. Bakker, R.G. Bacabac, A. Vatsa, S. Weinbaum, Mechanosensation and transduction in osteocytes, Bone 54 (2013) 182–190.

[23] S.F. Huang, W.R. Chen, C.L. Lin, Biomechanical interactions of endodontically treated tooth implant-supported prosthesis under fatigue test with acoustic emission monitoring, Biomed. Eng. Online 15 (2016) 23.

[24] S. Kuroshima, P. Entezami, L.K. McCauley, J. Yamashita, Early effects of parathyroid hormone on bisphosphonate/steroid-associated compromised osseous wound healing, Osteoporos. Int. 25 (2014) 1141–1150.

[25] R. Bernhardt, E. Kuhlisch, M.C. Schulz, U. Eckelt, B. Stadlinger, Comparison of bone-implant contact and bone-implant volume between 2D-histological sections and 3D-SRμCT slices, Eur. Cell Mater. 23 (2012) 237–247. discussion 247–248..

[26] M.L. Bouxsein, S.K. Boyd, B.A. Christiansen, R.E. Guldberg, K.J. Jepsen, R. Müller, Guidelines for assessment of bone microstructure in rodents using micro-computed tomography, J. Bone Miner. Res. 25 (2010) 1468–1486.

[27] U.E. Pazzaglia, T. Congiu, E. Franzetti, M. Marchese, F. Spagnuolo, L. Di Mascio, G. Zarattini, A model of osteoblast-osteocyte kinetics in the development of secondary osteons in rabbits, J. Anat. 220 (2012) 372–383.

[28] R. Yang, C.M. Davies, C.W. Archer, R.G. Richards, Immunohistochemistry of matrix markers in Technovit 9100 New-embedded undecalcified bone sections, Eur. Cell Mater. 6 (2003) 57–71. discussion 71.

[29] Y. Noyama, T. Nakano, T. Ishimoto, T. Sakai, H. Yoshikawa, Design and optimization of the oriented groove on the hip implant surface to promote bone microstructure integrity, Bone 52 (2013) 659–667.

[30] K. Oyama, M. Motoyoshi, M. Hirabayashi, K. Hosoi, N. Shimizu, Effects of root morphology on stress distribution at the root apex, Eur. J. Orthod. 29 (2007) 113–117.

[31] P.V. Soares, L.V. Souza, C. Veríssimo, L.F. Zeola, A.G. Pereira, P.C. Santos-Filho, A.J. Fernandes-Neto, Effect of root morphology on biomechanical behaviour of premolars associated with abfraction lesions and different loading types, J. Oral Rehabil. 41 (2014) 108–114.

[32] S.J. Kloehn, Significance of root form as determined by occlusal stress, J. Am. Dent. Assoc. Dental Cosmos 25 (1938) 1099–1110.

[33] L.F. Bonewald, The amazing osteocyte, J. Bone Miner. Res. 26 (2011) 229–238.

[34] M. Sasaki, S. Kuroshima, Y. Aoki, N. Inaba, T. Sawase, Ultrastructural alterations of osteocyte morphology via loaded implants in rabbit tibiae, J. Biomech. 48 (2015) 4130–4141.

[35] R.R. Barros, M. Degidi, A.B. Novaes, A. Piattelli, J.A. Shibli, G. Iezzi, Osteocyte density in the peri-implant bone of immediately loaded and submerged dental implants, J. Periodontol. 80 (2009) 499–504.

[36] A. Piattelli, L. Artese, E. Penitente, F. Iaculli, M. Degidi, C. Mangano, J.A. Shibli, P.G. Coelho, V. Perrotti, G. Iezzi, Osteocyte density in the peri-implant bone of implants retrieved after different time periods (4 weeks to 27 years), J. Biomed. Mater. Res. B Appl. Biomater. 102 (2014) 239–243.

[37] H.M. Frost, Bone's mechanostat: a 2003 update, Anat. Rec. A Discovery Mol. Cell Evol. Biol. 275 (2003) 1081–1101.

[38] H.M. Frost, A 2003 update of bone physiology and Wolff's Law for clinicians, Angle Orthod. 74 (2004) 3–15.

[39] D. Kaspar, W. Seidl, C. Neidlinger-Wilke, A. Beck, L. Claes, A. Ignatius, Proliferation of human-derived osteoblast-like cells depends on the cycle number and frequency of uniaxial strain, J. Biomech. 35 (7) (2002) 873–880.

[40] M.A. Peake, L.M. Cooling, J.L. Magnay, P.B. Thomas, A.J. El Haj, Selected contribution: regulatory pathways involved in mechanical induction of c-fos gene expression in bone cells, J. Appl. Physiol. (1985) 89 (6) (2000) 2498–2507.

[41] C.T. Rubin, L.E. Lanyon, Regulation of bone formation by applied dynamic loads, J. Bone Joint Surg. Am. 66 (3) (1984) 397–402.

[42] W.A. Weijs, H.J. de Jongh, Strain in mandibular alveolar bone during mastication in the rabbit, Arch. Oral Biol. 22 (1977) 667–675.

[43] A.I. Peptan, A. Lopez, R.A. Kopher, J.J. Mao, Responses of intramembranous bone and sutures upon in vivo cyclic tensile and compressive loading, Bone 42 (2008) 432–438.

[44] C. Slotte, D. Lundgren, L. Sennerby, A.K. Lundgren, Surgical intervention in enchondral and membranous bone: intraindividual comparisons in the rabbit, Clin. Implant Dent. Relat. Res. 5 (2003) 263–268.

[45] U. Breine, B. Johansson, P.J. Roylance, H. Roeckert, J.M. Yoffey, Regeneration of bone marrow. A Clinical and experimental study following removal of bone marrow by curettage, Acta Anat. (Basel) 59 (1964) 1–46.

[46] G. Danckwardt-Lillieström, Reaming of the medullary cavity and its effect on diaphyseal bone. A fluorochromic, microangiographic and histologic study on the rabbit tibia and dog femur, Acta Orthop. Scand. Suppl. 128 (1969) 1–153.

[47] W.T. Kim, Y.D. Cha, S.J. Oh, S.S. Park, H.W. Kim, The three dimensional finite element analysis of stress according to implant thread design inder the axial load, J. Korean Assoc. Oral Maxillofac. Surg. 27 (2001) 111–117.

[48] J. Steigenga, K. Al-Shammari, C. Misch, F.H. Nociti, H.L. Wang, Effects of implant thread geometry on percentage of osseointegration and resistance to reverse torque in the tibia of rabbits, J. Periodontol. 75 (9) (2004) 1233–1241.

[49] J. Hall, P. Miranda-Burgos, L. Sennerby, Stimulation of directed bone growth at oxidized titanium implants by macroscopic grooves: an in vivo study, Clin. Implant Dent. Relat. Res. 7 (2005) S76–S82.

[50] H.I. Yoon, I.S. Yeo, J.H. Yang, Effect of a macroscopic groove on bone response and implant stability, Clin. Oral Implants Res. 21 (2010) 1379–1385.

[51] S.F. Hulbert, F.A. Young, R.S. Mathews, J.J. Klawitter, C.D. Talbert, F.H. Stelling, Potential of ceramic materials as permanently implantable skeletal prostheses, J. Biomed. Mater. Res. 4 (1970) 433–456.

[52] Y. Kuboki, Q. Jin, H. Takita, Geometry of carriers controlling phenotypic expression in BMP-induced osteogenesis and chondrogenesis, J. Bone Joint Surg. Am. 83 (2001) S105–S115.

[53] E. Tsuruga, H. Takita, H. Itoh, Y. Wakisaka, Y. Kuboki, Pore size of porous hydroxyapatite as the cell-substratum controls BMP-induced osteogenesis, J. Biochem. 121 (1997) 317–324.

[54] H.E. Götz, M. Müller, A. Emmel, U. Holzwarth, R.G. Erben, R. Stangl, Effect of surface finish on the osseointegration of laser-treated titanium alloy implants, Biomaterials 25 (2004) 4057–4064.

[55] Q.M. Jin, H. Takita, T. Kohgo, K. Atsumi, H. Itoh, Y. Kuboki, Effects of geometry of hydroxyapatite as a cell substratum in BMP-induced ectopic bone formation, J. Biomed. Mater. Res. 51 (2000) 491–499.

[56] Y. Kuboki, Q. Jin, M. Kikuchi, J. Mamood, H. Takita, Geometry of artificial ECM: sizes of pores controlling phenotype expression in BMP-induced osteogenesis and chondrogenesis, Connect. Tissue Res. 43 (2002) 529–534.

[57] J.T. Steigenga, K.F. al-Shammari, F.H. Nociti, C.E. Misch, H.L. Wang, Dental implant design and its relationship to long-term implant success, Implant Dent. 12 (4) (2003) 306–317.

[58] T. Ishimoto, T. Nakano, Y. Umakoshi, M. Yamamoto, Y. Tabata, Degree of biological apatite c-axis orientation rather than bone mineral density controls mechanical function in bone regenerated using recombinant bone morphogenetic protein-2, J. Bone Miner. Res. 28 (2013) 1170–1179.

[59] S. Tatsumi, K. Ishii, N. Amizuka, M. Li, T. Kobayashi, K. Kohno, M. Ito, S. Takeshita, K. Ikeda, Targeted ablation of osteocytes induces osteoporosis with defective mechanotransduction, Cell Metab. 5 (6) (2007) 464–475.